Late Quaternary palaeoclimatic oscillations in East Africa recorded by heavy minerals in the Nile delta

Alain Foucault* & Daniel Jean Stanley†

* Laboratoire de Géologie, Muséum national d'Histoire naturelle, 75005 Paris, France
† Mediterranean Basin Program, Smithsonian Institution, Washington DC 20560, USA

BECAUSE the Nile carries a load derived from markedly different geological terrains and climatic zones, it is expected that mineralogical study of deposits in its delta could help define changes in palaeoclimate affecting East Africa. Here we report measurements on heavy minerals in the Nile delta which can be used as distinct markers of climatic shifts over Africa during the late Pleistocene to Recent. Variations of heavy minerals in radiocarbon-dated cores collected in this delta[1], the Nile's major depocentre[2], correlate closely with oscillations in African palaeoclimate determined by other independent methods, such as studies of lake levels. These variations are largely a function of the characteristics of the Nile. It flows across nearly 35° of latitude, from south of the Equator to the Mediterranean (Fig. 1*a*), and conditions in its drainage basin, which includes central Africa, the Ethiopian plateau and eastern Sahara, range from a tropical, humid to a warm, arid climate. East African climatic belts migrated considerably during the Quaternary[3–5], modifying Nile discharge and sediment load. Climatic oscillations have been recorded by changes of sediment yield and grain size along its course[6,7] and by well defined depositional cycles[8], including sapropels[9], in the eastern Mediterranean.

The Main Nile, north of 18° N latitude, comprises flow from three major tributaries: the White Nile, Blue Nile and Atbara river (Fig. 1*b*). At present, their hydrology and sediment load are markedly different[10] (Fig. 2). The White Nile contributes almost a third of the total discharge, but only a minor proportion of sediment; pyroxene is almost absent, whereas amphibole, eroded from metamorphic terrains, accounts for a high proportion of the transparent heavy minerals suite[11]. The Blue Nile contributes more than half of the Main Nile discharge and almost three-quarters of the sediment load; the proportion of pyroxene relative to amphibole is high[11]. The Atbara contributes only a small part of the total discharge but one quarter of the Main Nile sediment load; pyroxene is much more abundant than amphibole[11]. Differences in discharge of these three tributaries are a function of different surface areas of their respective drainage basins and differences in rainfall (Fig. 1*a*, *b*). Differences in sediment load record seasonal variations in rainfall[10,12] and vegetal cover[13] in the various basins. Differences in composition of sediments in the three tributaries are due to markedly different geological formations eroded in the Ethiopian highlands and central African plateau[14].

In contrast to the negligible amounts of pyroxene carried by the White Nile is the high proportion of pyroxene in the Blue Nile and even higher proportions in the Atbara. These high proportions result from erosion of Ethiopian volcanic terrains. Pyroxene and amphibole, with a roughly comparable specific gravity and weathering stability index[15], generally constitute more than 50% of the total heavy mineral suite in Main Nile samples. It should thus be possible to evaluate changes in the sediment load contributed by each of the three main tributaries by studying the relative proportions of these heavy minerals carried by the Main Nile. The relative proportion of amphibole to pyroxene has been calculated using a standardized index (ratio) applied to compare deposits in the various Nile river tributaries. This index was defined by Hassan[16]: $I\text{Amph} =$ (frequency of amphibole/frequency of amphibole + pyroxene) $\times$ 100. Sand fractions were selected for study from 73 core samples of late Pleistocene and Holocene age in the Lake Manzala region of the eastern Nile delta (Fig. 1*c*), including cores S6, S7, S8 and S22[1,17]. Cores S7 and S22 are somewhat coarser and provide larger numbers of samples (29 from S7, and 28 from S22) containing heavy minerals of sand size grains coarser than 63 μm. At least 300 heavy mineral grains (63–250 μm in size) were identified in each sample using standard petrographic microscope techniques. We have prepared a tabulated list of heavy mineral percentages and *I*Amph values for all studied core samples (available from the authors).

Core S7 is stratigraphically more complete and comprises four major stratigraphic units, from the base upwards (Fig. 3): IV—fluvial sands, 24.5–19.3 m from the core top; III—oxidized silty muds of interchannel, sebkha and/or swamp origin, 19.3–14.7 m; II—fluvial and coastal sands, 14.7–10 m; and I—marine delta-front muds, coastal sands (5–4 m) and subaerial deltaic sequences at the core top. Unit I represents the recent progradational delta. Radiocarbon dates indicate that units IV, III and II are upper Pleistocene (IV and III from about 40,000 to 20,000 yr BP; II from about 20,000 to 12,000–10,000 yr BP). Unit I, mid- to upper-Holocene, ranges from about 8,000 yr BP to the Present. A depositional hiatus occurs between 12,000–10,000 and 8,000 yr BP[17].

The relative proportions of amphibole and pyroxene, as measured by the *I*Amph index, vary considerably from the base to the top of core S7 (Fig. 3). In units IV and III, *I*Amph values average 63.4 ± 5 (numbers after $\pm$ refer to 1 standard deviation). In unit II, the index is 35.7 ± 7. In unit I, index values increase initially (76.8 ± 20 between 8.2 and 5.8 m; maximum value of 96), and then decrease markedly further up (38.0 ± 11 between 5.5 m and the core top). Note that there is no correlation between *I*Amph values and specific lithofacies or grain size, indicating that the proportion of the two minerals in this core is controlled by factors other than local hydrodynamic processes.

Core S22, longer than S7, comprises a thicker Holocene section (unit I) but does not include unit IV (Fig. 3). Unit III forms the base (from 38.8 to 37.7 m) and unit II occurs from

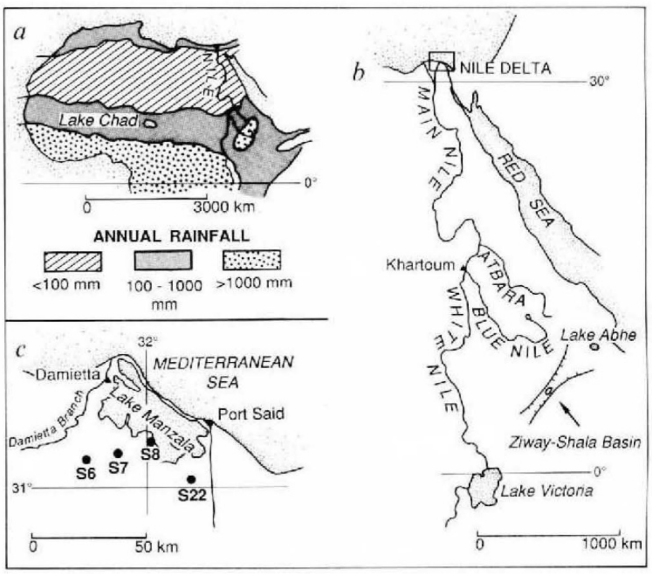

FIG. 1 *a*, Map showing position of the Nile river and Lake Chad, and annual rainfall on the African continent[13]. *b*, Map showing the Nile delta, Nile river and its tributaries, the Atbara and Blue Nile draining the Ethiopian plateau and White Nile draining the Central African plateau. Box indicates area in *c*. *c*, Map of the north-eastern Nile delta, showing the position of studied cores.

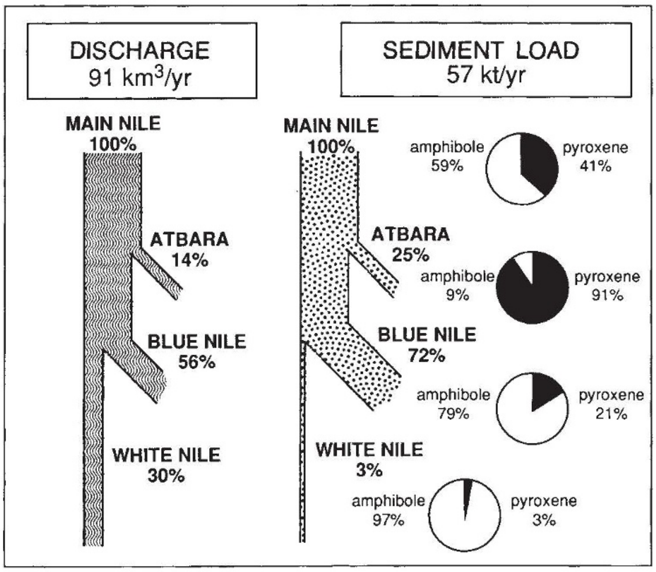

FIG. 2 Diagrams showing (left) the total Nile river discharge and relative proportions supplied from its three main tributaries, and (right) total sediment load and relative load proportions in the tributaries (compare ref. 10). Pie diagrams indicate the relative proportions of amphibole and pyroxene in the present bed-load of the Main Nile and its tributaries[11].

37.7 to 22 m; unit I constitutes more than half of the core length. A sand layer between 5 m and 3.2 m probably correlates with the sand section at 5-4 m in core S7. In unit II, *I*Amph index values average 29.6 ± 6. In unit I, heavy minerals are absent in fine-grained muds between 22 m and 15 m; above this, *I*Amph values are initially low (29.7 ± 13 between 15 and 8 m) but then increase (67.2 ± 13; maximum value of 84.5) between 8 and 4.5 m. Deposits at the top of the core reveal an *I*Amph index of 44.2 ± 9. The overall pattern of the *I*Amph values parallels that in core S7; some differences may be due to local reworking by coastal currents on the delta margin to cause removal of less dense minerals and concentrate opaque heavy minerals[18], which occurred, for example, to an extent of >75% between 14.5 and 6 m.

There are fewer sandy samples with heavy minerals in cores S6 and S8[19], but *I*Amph index patterns in these two cores are consistent with those of time-equivalent sections in S7 and S22. Also calculated are *I*Amph values in sandy samples from two suites of cores further to the west in the Nile delta, in the Damietta and Rosetta promontories[20]. Values in these cores, available only for the upper parts of units II and I, are comparable to those of cores S7 and S22.

Patterns of *I*Amph values are not random but vary during specific time periods (Fig. 3). We attribute these distinct time-related variations to changes in the relative sediment load contributions from major Nile tributaries. Studies of time-related changes of sediment yield and grain size during the late Quaternary[7] show that the load of the Blue Nile and Atbara, both primary sources of pyroxene in the Main Nile, varied considerably during this period. The large load presently carried by these two rivers results from the interplay of seasonal, and often intense, rainfall (primarily during summer) affecting an arid region with moderate to low vegetation cover over most of the Ethiopian drainage basin area[10,12,13]. It is probable that more humid phases affecting this region would have given rise to a longer rainy season and denser vegetation cover. An increased vegetal cover reduces erosion and removal of sediments. Thus, wetter conditions would have resulted in decreased sediment loads carried by both Ethiopian tributaries, even if their discharge were to have increased[7]. This decreased sediment load would result in a decreased supply of pyroxene to the Main Nile and, in consequence, an increased *I*Amph value. This increase would have been particularly important at times of extended vegetal cover over the Atbara drainage basin, the main source of pyroxenes.

White Nile load fluctuations are also affected by changing climatic/geographical factors, and so would also have induced changes in proportions of heavy minerals, for example during times of cut-off from Uganda headwaters before ~12,500 yr BP[6]. Even if the discharge of the White Nile were to have increased considerably, its load would have remained generally low because of a more constant vegetation cover on its drainage basin during most of the late Quaternary[21,22]. The White Nile sediment contribution became relatively much more important when loads of the Blue Nile and Atbara decreased during humid phases. Simplified calculations using the Nile hydrological data in Fig. 2 suggest, for example, that *I*Amph values of ~80 imply equivalent sediment loads from the While Nile and Ethiopian tributaries.

Thus, decreased proportions of pyroxene (that is, an increase in *I*Amph values) in sediments of the Main Nile and in the delta would indicate an increased vegetation cover in the drainage basins of the Blue Nile and the Atbara, and consequently,

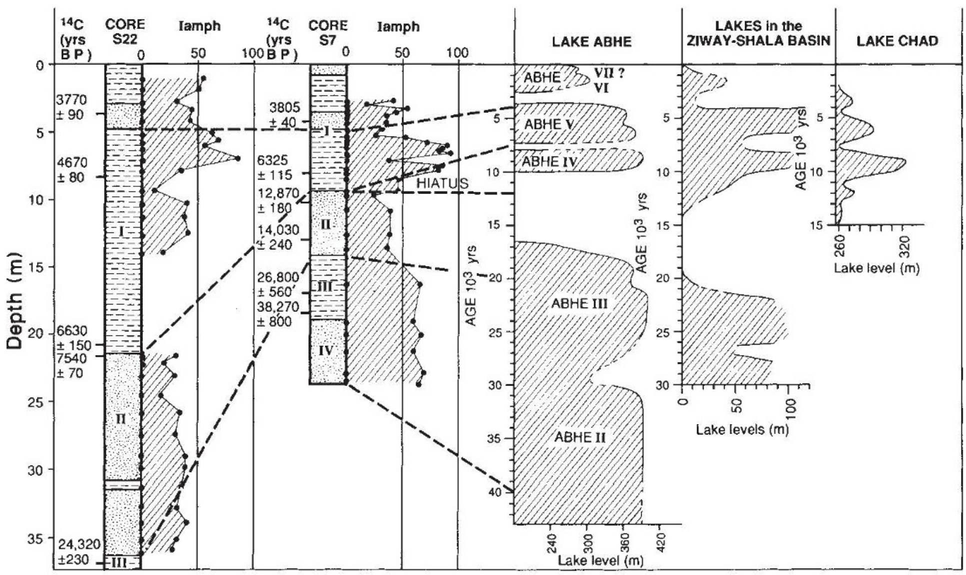

FIG. 3 *I*Amph index patterns plotted along radiocarbon-dated lithostratigraphic sections of cores S22 and S7. I to IV corresponds to stratigraphic units discussed in text. Time correlation indicated by dashed lines. *I*Amph patterns are correlated with lake level variations, including those of Lake Abhe[23], lakes in the Ziway-Shala[24] Basin and Lake Chad[25].

more humid conditions. At such times it is also probable that tributaries (now dry), draining extensive areas and coming in from the desert along the western flank of the Main Nile, yielded more amphibole than pyroxene (D. A. Livingstone, personal communication). On the other hand, increased proportions of pyroxene transported to the Main Nile (that is, a decrease in *I*Amph values) would probably indicate a reduction of vegetation cover, accentuated erosion of the Ethiopian plateau and thus more arid conditions. Moreover, some fluctuations recorded in cores probably reflect temperature and rainfall oscillations. Lower temperatures may cause an increase in loads contributed by the Atbara and Blue Nile as a result of solifluction, lowered tree-lines and increased hillside-slope instability (M. A. J. Williams, personal communication).

These interpretations can be evaluated in the light of late Quaternary palaeoclimatological studies that use other techniques, such as the measurement of African lake levels (Fig. 3). The temporal pattern of the *I*Amph index in core S7 correlates, for example, with changes of level of Lake Abhe east of the Ethiopian plateau[23], and lakes in the Ziway-Shala Basin in the Ethiopian Rift[24] (Figs 1*b* and 3). High *I*Amph values in units IV and III (~40,000-20,000 yr BP) correspond to periods of high lake levels recorded before about 20,000-17,000 yr BP. Low *I*Amph values in unit II (~20,000 to 12,000-10,000 yr BP) correlate with low lake levels from about 20,000-17,000 to 14,000-10,000 yr BP. *I*Amph values which increase and then decrease upward in unit I, between 10 and 5.5 m from the core top, span a period of high lake levels between 7,000 and 4,000 yr BP. The increased *I*Amph values at ~3.4 m may be related to the climatic phases that induced high lake levels found for ~1,500 yr BP.

In summary, heavy minerals suites in dated Quaternary Nile delta deposits serve not only as provenance markers[11,19] but also as valuable indicators of East African palaeoclimatic oscillations. Pronounced time-related changes in proportions of pyroxene are directly related to climatic oscillations over the Ethiopian plateau, and to very large changes in sediment loads of major Nile tributaries. These changes were probably associated with larger-scale north-south displacements of climatic belts across extensive sectors of the African continent. This is supported by correlations of Nile delta compositional data with variations of lake levels in distant regions, such as Lake Chad[25] (Fig. 3) located at about the same latitude and about 3,000 km west of the Ethiopian plateau (Fig. 1*a*). Study of heavy minerals in dated sedimentary sequences holds promise as an independent criterion to be used in conjunction with other methods to interpret regional palaeoclimatic oscillations. □

Received 28 November 1988; accepted 9 March 1989.

1. Stanley, D. J. *Science* **240**, 497-500 (1988).
2. Said, R. *The Geological Evolution of the River Nile* (Springer, New York, 1981).
3. Livingstone, D. A. *A. Rev. Ecol. Systematics* **6**, 249-280 (1975).
4. Williams, M. A. J. & Faure, H. (eds) *The Sahara and The Nile: Quaternary Environments and Prehistoric Occupation in Northern Africa* (Balkema, Rotterdam, 1980).
5. Hamilton, A. *Environmental History of East Africa. A Study of the Quaternary* (Academic, London, 1982).
6. Williams, M. A. J. & Adamson, D. A. in *The Sahara and The Nile: Quaternary Environments and Prehistoric Occupation in Northern Africa.* (eds Williams, M. A. J. & Faure, H.) 281-304 (Balkema, Rotterdam, 1980).
7. Adamson, D. A., Gasse, F., Street, F. A. & Williams, M. A. J. *Nature* **288**, 50-55 (1980).
8. Stanley, D. J. & Maldonado, A. *Nature* **266**, 129-135 (1977).
9. Rossignol-Strick, M., Nesteroff, W., Olive, P. & Vergnaud-Grazzini, C. *Nature* **295**, 105-110 (1982).
10. Hurst, H. E. *The Nile: A General Account of the River and the Utilization of its Waters* 2nd edn (Constable, London, 1957).
11. Shukri, N. M. *Q. J. geol. Soc. Lond.* **105**, 511-534 (1950).
12. Griffiths, J. F. (ed.) *Climates of Africa: World Survey of Climatology* Vol. 10 (Elsevier, Amsterdam, 1972).
13. Van Chi-Bonnardel, R. *The Atlas of Africa* (The Free Press, New York, 1973).
14. UNESCO *Tectonics of Africa* (UNESCO, Paris, 1971).
15. Pettijohn, F. J. *Sedimentary Rocks* 2nd edn (Harper & Brothers, New York, 1957).
16. Hassan, F. A. *Quat. Res.* **6**, 425-443 (1976).
17. Coutellier, V. & Stanley, D. J. *Mar. Geol.* **77**, 257-275 (1987).
18. Hilmy, M. E. *J. sedim. Petrol.* **21** (2) 109-120 (1951).
19. Stanley, D. J., Sheng, H. & Pan, Y. *J. Afr. Earth Sci.* **7**, 735-741 (1988).
20. El Askary, M. A. & Frihy, O. E. *Bull. Fac. Sci. Alexandria Univ.* (in the press).
21. Livingstone, D. A. in *The Sahara and The Nile: Quaternary Environments and Prehistoric Occupation in Northern Africa.* (eds Williams, M. A. J. & Faure, H.) 339-359 (Balkema, Rotterdam, 1980).
22. Bonnefille, R. & Riollet, G. *Quat. Res.* **30**, 19-35 (1988).
23. Gasse, F. *Nature* **265**, 42-45 (1977).
24. Gasse, F. & Street, F. A. *Palaeogeog. Palaeoclimatol. Palaeoecol.* **34**, 279-325 (1978).
25. Servant, M. & Servant-Vildary, S. in *The Sahara and The Nile: Quaternary Environments and Prehistoric Occupation in Northern Aftrica.* (eds Williams, M. A. J. & Faure, H.) 133-162 (Balkema, Rotterdam, 1980).

ACKNOWLEDGEMENTS. We thank Mr H. Sheng for assistance with the heavy mineral analyses, and Drs H. R. Davis, H. Faure, D. A. Livingstone, M. Servant and M. A. J. Williams for their reviews. This study, part of the Mediterranean Basin (MEDIBA) Program (D.J.S.) and "Evolution des climats et sédimentation" program (A.F.), was funded by grants from the Smithsonian Scholarly Studies Program, AMOCO Production Company, the National Geographic Society and the Muséum national d'Histoire naturelle.

Molecular evidence for pre-Cretaceous angiosperm origins

William Martin, Alfons Gierl & Heinz Saedler

Max-Planck-Institut für Züchtungsforschung,
Abteilung Molekulare Pflanzengenetik, D-5000 Köln 30, FRG

FLOWERING plants or angiosperms have dominated the Earth's flora since at least the late Cretaceous[1] and were already highly diversified by Barremian times, about 120 million years (Myr) ago. However, because of the paucity of fossilized angiosperm reproductive structures from lower Cretaceous sediments[2,3] and the absence of generally recognized angiosperm fossils from pre-Cretaceous strata[4,5], their origins and early evolution remain obscure. Similarly, attempts to understand pre-Cretaceous angiosperm evolution[4-11] have been impaired by difficulties in defining and interpreting angiospermous characters in fossil specimens[8,12]. We report here molecular evidence suggesting that angiosperm ancestors underwent diversification more than 300 Myr ago.

To obtain a molecular view of angiosperm origins we have determined nucleotide sequences for full-size complementary DNAs of a slowly evolving glycolytic enzyme, glyceraldehyde-3-phosphate dehydrogenase (GAPDH), from six flowering plants. The six nucleotide sequences from animals[13,14], one from yeast[15], and nine from plants (this study and refs 16-18) yielded, upon alignment, 332 codons for comparison in each of the 16 coding regions. Divergence was measured with the weighted pathway method[19]. Pairwise comparisons between organisms for which divergence times are roughly known reveal that the nonsynonymous substitution rate (K_a) of GAPDH has remained constant along separate eukaryotic lineages (Table 1). Were the nonsynonymous rate for GAPDH within angiosperms or their antecedents markedly accelerated relative to that in animals, we would expect values of K_a for comparisons involving plants to exceed those for animals versus yeast. Yet the yeast outgroup reveals that the nonsynonymous rate for GAPDH in plants may be slightly (7%) lower than that in animals. Eukaryotic GAPDH sequences are at compositional equilibrium[20] for first and second codon positions (data not shown); values of K_a in comparisons between angiosperm GAPDH sequences should thus provide reasonable estimates for the timescale of angiosperm evolution.

Numbers of nonsynonymous and synonymous substitutions per site (K_a and K_s, respectively) for comparisons between angiosperm GAPDH sequences are shown in Table 2. Included in the table are the corresponding values for comparisons of full-size complementary DNA sequences for chalcone synthase (CHS), the key enzyme of anthocyanin biosynthesis, from seven[21] of the nine angiosperms considered here. The parallel analysis of enzymes from primary (GAPDH) and secondary (CHS) metabolic pathways contributes significantly to the elimination of potential errors inherent in phylogenetic inferences based upon a single gene. For these two nuclear genes and the seven species from which both sequences have been determined, average divergence at synonymous and nonsynonymous sites between monocots and dicots consistently exceeds that within